

Supporting Information

Self-powered 2D-material sensing system driven by SnSe piezoelectric nanogenerator

Peng Li*¹, Zekun Zhang¹, Wangtian Shen¹, Chunguang Hu^{2,3}, Wanfu Shen*^{2,3}, Dongzhi
Zhang*⁴

1. State Key Laboratory of Precision Measurement Technology and Instruments, Department of Precision Instruments, Tsinghua University, Beijing 100084, China.
2. College of Precision Instrument and Optoelectronics Engineering, Tianjin University, Tianjin 30072, China.
3. State Key Laboratory of Precision Measuring Technology and Instruments, Tianjin University, NO.92 Weijin Road, CN-300072 Tianjin, China.
4. College of Control Science and Engineering, China University of Petroleum (East China), Qingdao 266580, China.

1. Asymmetric output signals of SnSe PENG
2. Constructively/destructively connecting two SnSe nanogenerators in series
3. Output properties of bare PET substrate
4. I-V measurements of SnSe crystal along two orthogonal principle axes
5. Energy harvesting performance of SnSe PENG from human body
6. I-V characteristic of MoS₂ sensor
7. MoS₂ photodetector driven by mechanical energy from pulse
8. Response of MoS₂ humidity sensor to heat source
9. Relation between MoS₂ relative resistance change and humidity
10. HRTEM image of SnSe
11. Photo of integrated device

1. Asymmetric output signals of SnSe PENG

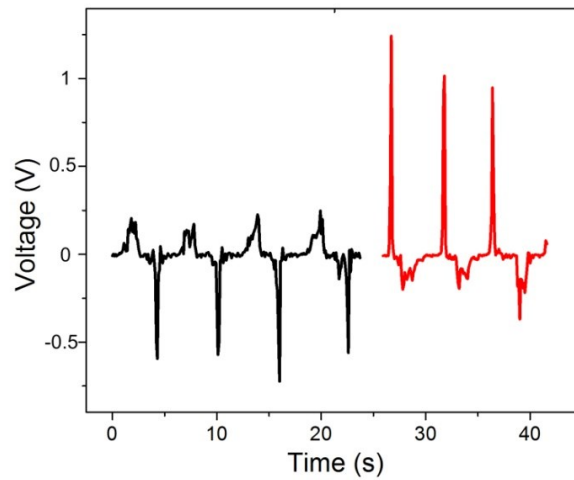


Figure S2. The magnitude of output voltages depends on the bending/releasing rate. Asymmetric output signals can be observed when the bending rate of SnSe PENG is larger/smaller than releasing rate.

2. Constructively/destructively connecting two SnSe nanogenerators in series

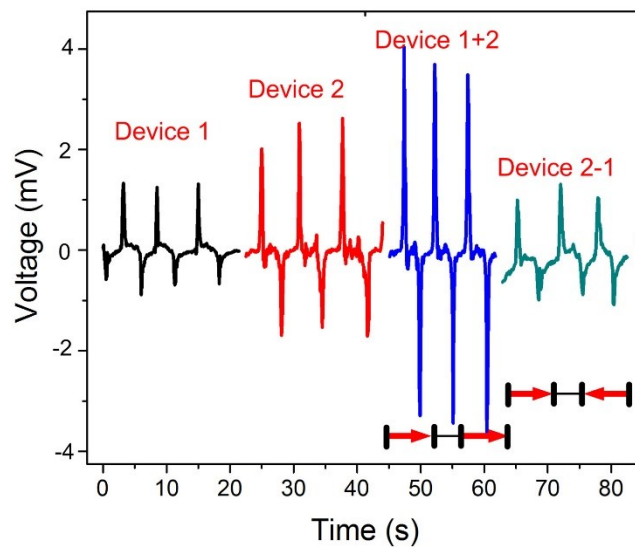


Figure S2. Output performance of two SnSe nanogenerators (constructively/destructively) connected in series.

3. Output properties of bare PET substrate

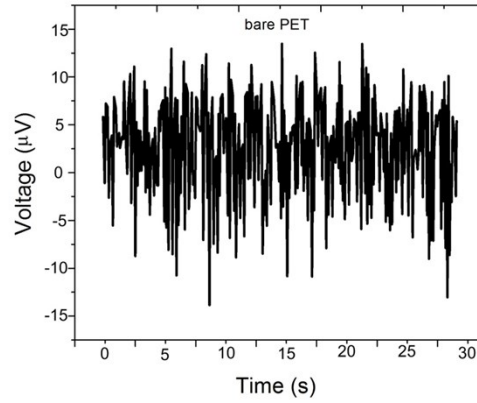


Figure S3. No output signal was observed from bare PET substrates without SnSe flake.

4. I-V measurements of SnSe crystal along two orthogonal principle axes

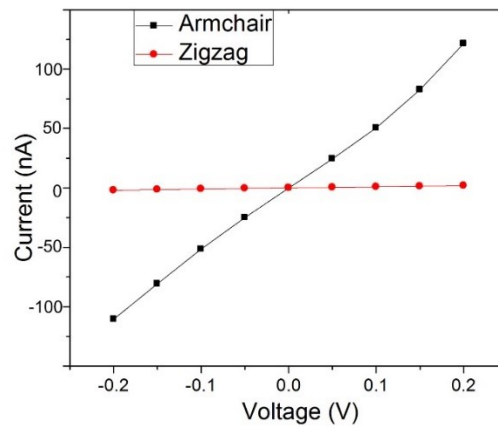


Figure S4. I-V characteristics of SnSe along armchair/zigzag direction.

5. Energy harvesting performance of SnSe PENG from human body

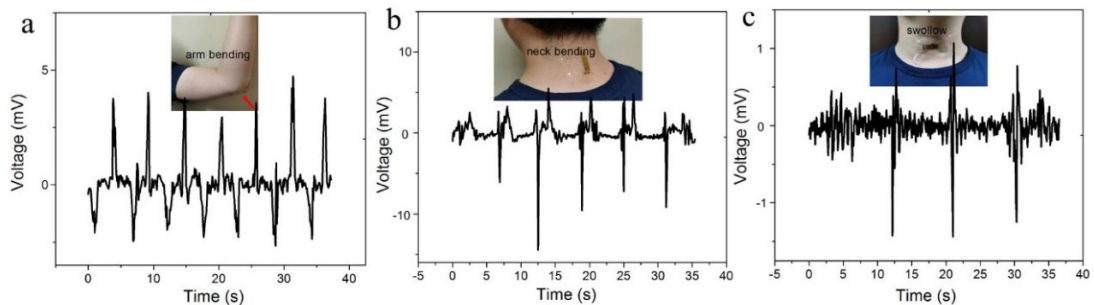


Figure S5. Energy harvesting of SnSe PENG from arm bending (a), neck bending (b), and swallowing (c).

6. I-V characteristic of MoS₂ sensor

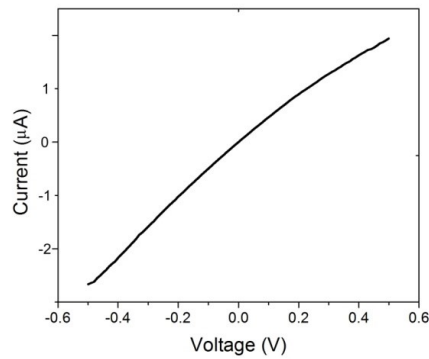


Figure S6. The I-V curve of a typical MoS₂ device, which demonstrates good linearity.

7. MoS₂ photodetector driven by mechanical energy from pulse

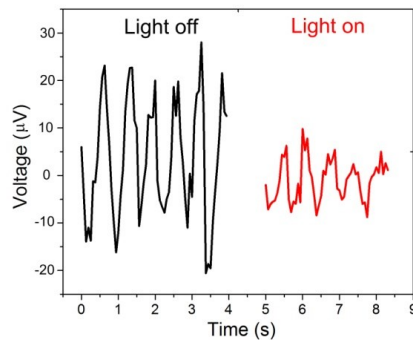


Figure S7. Pulse is used to power the SPNS. After illumination, the voltage across the MoS₂ sensor reduced from 20 μV to ~10 μV.

8. Response of MoS₂ humidity sensor to heat source

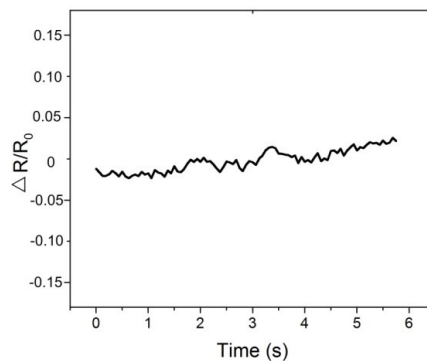


Figure S8. In order to prove that the local humidity change instead of temperature change is the major factor that causes the resistance variation when the finger approaches MoS₂ sensor, we used a heat source which temperature was ~40 °C to approach MoS₂ sensor with distance of 5 mm. As a result, the sensor showed negligible response (<0.05).

9. Relation between MoS₂ relative resistance change and humidity

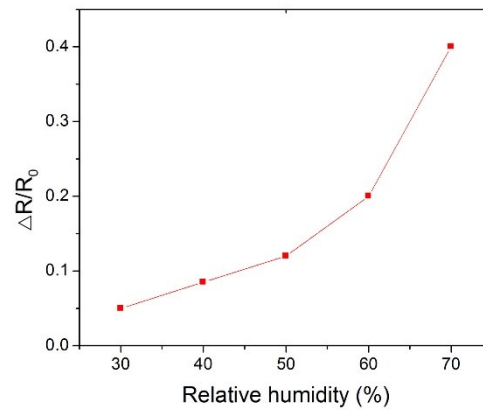


Figure S9. Relation between MoS₂ relative resistance change and humidity.

10. HRTEM image of SnSe

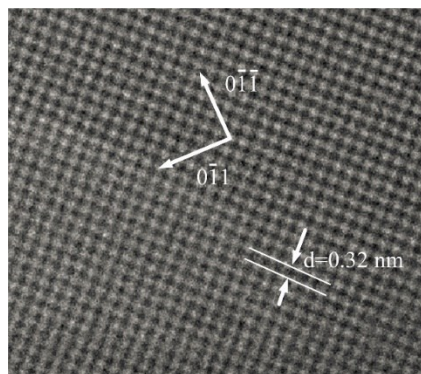


Figure S10. HRTEM image of SnSe.

11. Photo of integrated device

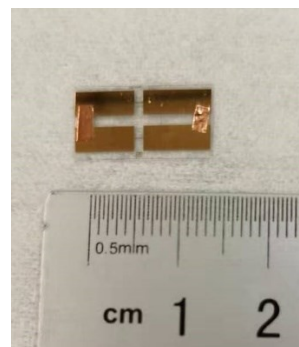


Figure S11. Photo of integrated device.